

Green and Self-Lubricating Polyoxymethylene Composites Filled with Low-Density Polyethylene and Rice Husk Flour

Ke Li, Dinghan Xiang, Xiaoyu Lei

College of Materials Science and Technology, Nanjing University of Aeronautics and Astronautics, Nanjing 210016, China

Received 22 August 2007; accepted 24 September 2007

DOI 10.1002/app.27603

Published online 25 February 2008 in Wiley InterScience (www.interscience.wiley.com).

ABSTRACT: Polyoxymethylene (POM) composites filled with low-density polyethylene (LDPE) and rice husk flour (RHF) were prepared by injection molding. The POM/5 wt % LDPE/7.5 wt % RHF composite exhibited the lowest wear rate, whereas the coefficient of friction remained low, and the POM/5 wt % LDPE/5 wt % RHF composite had the best mechanical properties. X-ray diffraction analysis was carried out, and the worn surfaces were examined with scanning electron microscopy. The results showed that the addition of the filler reduced the crystallinity degree of the POM composites. The main wear

mechanism for unfilled POM was adhesion, whereas for the POM composites, wear seemed to occur mainly by fatigue and abrasion. It was experimentally confirmed that the POM composite filled with LDPE and RHF, which is well-performing, low-cost, and environmentally friendly, could be a potential material for tribological applications. © 2008 Wiley Periodicals, Inc. *J Appl Polym Sci* 108: 2778–2786, 2008

Key words: composites; high performance polymers; injection molding; mechanical properties; recycling

INTRODUCTION

Ecological concern has recently resulted in a renewed interest in natural materials, and issues such as recyclability and environmental safety have become increasingly important for the introduction of new materials and products.¹ In Europe, new environmental legislation has been passed by the European Parliament that requires manufacturers of materials and end products to consider the environmental impact of their products at all stages of their lifecycle, including ultimate disposal.² These environmental issues in combination with their low cost have recently generated considerable interest in natural fibers, such as jute, sisal, coir, flax, wood flour, and rice husk flour (RHF).^{3–6} Natural fibers provide a number of advantages over traditional synthetic fibers such as glass fibers and carbon fibers. They are (1) low density, (2) high specific strength and modulus, (3) relative non-abrasiveness to processing equipment, (4) wide availability, (5) cheapness, (6) renewability, (7) biodegradability, (8) CO₂ neutrality (when burned), and (9) energy recovery (when incinerated).

The combination of good mechanical and physical properties together with their environmentally

friendly character makes natural fibers extremely possible alternatives for traditional synthetic fibers in engineering composites. Developments in natural fibers in the past few years have shown that it is possible to obtain well-performing natural fiber/polymer composites.^{7–11} These so-called green composites, with environmentally friendly and low-cost characters, have found applications in many industries, especially in the automotive and construction industries.¹²

Polyoxymethylene (POM) is a widely used material in many tribological applications because of its excellent friction and wear properties. To further enhance its tribological behavior and broaden its application, various fillers, such as polytetrafluoroethylene (PTFE), MoS₂, glass fibers, and carbon fibers, have been incorporated into POM as internal lubricants or reinforcements by many researchers.^{13–15} However, little consideration has been given to the problem of environmental pollution and cost control when POM is filled with these fillers. For example, many POM products for tribological applications include PTFE as an internal lubricant, which will exert an unfavorable impact on our environment at the end of their life cycle because of the existence of fluorine. The high price of PTFE also increases the cost of the POM products. Therefore, it is of great significance to find other materials as substitutes for these traditional fillers while maintaining the excellent properties of POM products.

Correspondence to: D. Xiang (xiangdh@nuaa.edu.cn).

In this investigation, low-density polyethylene (LDPE), which possesses a low friction coefficient and does not contain any element harmful to the environment, was selected as the internal lubricant to take the place of traditional lubricants such as PTFE and MoS_2 . In the mean time, RHF, a kind of readily available natural fiber, was used as the reinforcement because of its characteristics mentioned previously. The end-of-life incineration of natural fibers results in recovered energy. This work aims to produce a polymer composite that is well-performing, low-cost, and environmentally friendly. It is also hoped that this work will be helpful in understanding the effect of natural fibers on the mechanical and tribological properties of POM composites.

EXPERIMENTAL

Materials and sample preparation

The matrix polymer material used was a POM copolymer (M90) provided by Yunnan Yuntianhua Co. (Yunnan, China). LDPE (Q/3201-BYC-01, Bycolene), used as the internal lubricant, was supplied by BASF-YPC Co. (Nanjing, China). RHF was obtained from ground rice husks through a 60-mesh sieve.

The pelletized POM and LDPE were dried in an electric oven at 85°C for 2 h, and RHF was dried at 95°C for 24 h to remove water before extrusion. The materials were then weighed in the required proportions, and the mixture was blended with a high-speed mixer. After that, the polymer blends were produced with a reciprocating single-screw extruder (diameter = 30 mm, length/diameter = 20; CM-30, Nanjing Chengmeng Chemical Machine Co., Nanjing, China). The temperatures maintained in the five zones of the extruder barrel were 160, 180, 190, 195, and 185°C . The screw speed was set at 20 rpm. The extrudate was obtained in the form of a cylindrical rod that was quenched in cold water and then pelletized.

For making the specimens for mechanical and tribological tests, the pelletized polymer blends were put in a cuboidal mold ($85 \times 47 \times 46 \text{ mm}^3$) made of 1Cr18Ni9Ti, which was heated to 175°C . After the blends melted, a maximum pressure of 20 MPa was applied to expel the entrapped air out of the mold. Then, the heat was turned off, and the molded blends were left to cool in the mold under pressure for 30 min before it was opened. Afterwards, a molded slab with a size of $85 \times 47 \times 10 \text{ mm}^3$ was obtained. Two specimens for tribological tests with a size of $43 \times 36 \times 10 \text{ mm}^3$ were cut out of the molded slab. They were then finished by abrasion against 800-grit sandpaper to ensure good contact between the specimen surface and the counterface. The standard specimens for mechanical property

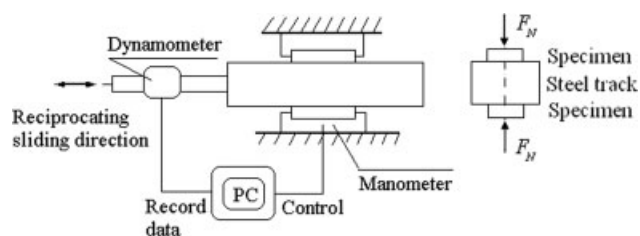


Figure 1 Schematic representation of the part related to the loading of the tribotester.

tests were made through machine work on the molded slab.

Mechanical property tests

The tests of the compressive properties were performed with a universal testing machine (New Sansy Co., Shenzhen, China) with a specimen of the size of $30 \times 10 \times 10 \text{ mm}^3$ according to GB/T 1041-92 at a loading speed of 5 mm/min. The tests of the impact strength were carried out according to GB/T 1043-79.

Friction and wear tests

Friction and wear tests were performed in a computer-controlled reciprocating sliding tribotester. A schematic diagram of the part related to the loading of the apparatus is shown in Figure 1. The counterface was made of 45 carbon steel with a chemical composition of 0.42–0.50 wt % carbon, 0.50–0.80 wt % manganese, and 0.17–0.37 wt % silicon. The counterface was polished with 1500-grit metallographic abrasive paper before the test. A dry sliding test was conducted under ambient conditions (temperature = $20 \pm 5^\circ\text{C}$, relative humidity = $60 \pm 5\%$) with a nominal pressure of 5 MPa and a reciprocating sliding frequency of 1.0 Hz. The stroke length was 14 mm. Before testing, the surfaces of the specimens and counterface were cleaned with acetone and thoroughly dried.

The friction force and normal load were measured from the output of linear variable strain gauges, and then the frictional coefficient was calculated and recorded automatically by the computer. During the test, the surface temperature of the specimen was monitored by a thermocouple that was inserted into a hole of 0.8 mm in the track close to the rubbing surface. Wear loss was measured gravimetrically with a precision balance to an accuracy of 0.1 mg after each test. The wear test for each condition was repeated two times, and the average values were reported. The results were within a scatter range of $\pm 15\%$. The sliding distance of each test was 300 m, which was enough to allow for the steady-state sliding period to be achieved. The specific wear rate [w_r ,

TABLE I
Mechanical Properties of POM and Its Composites

Sample	LDPE (wt %)	RHF (wt %)	Density (g/cm ³)	Compressive yield strength (MPa)	Compressive modulus (MPa)	Impact strength (kJ/m ²)
POM (A)	—	—	1.390	110.6	1377	6.3
POM/LDPE (A1)	2.5	—	1.375	96.8	1209	6.5
POM/LDPE (A2)	5	—	1.348	101.8	1314	7.2
POM/LDPE (A3)	7.5	—	1.321	105.1	1371	6.2
POM/LDPE (A4)	10	—	1.308	98.6	1203	5.3
POM/LDPE (A5)	12.5	—	1.284	92.1	1134	4.2
POM/LDPE/RHF (B1)	5	2.5	1.336	110.8	1488	6.6
POM/LDPE/RHF (B2)	5	5	1.327	117.2	1617	6.2
POM/LDPE/RHF (B3)	5	7.5	1.315	106.7	1455	5.7
POM/LDPE/RHF (B4)	5	10	1.299	89.2	1221	4.3
POM/LDPE/RHF (B5)	5	12.5	1.283	79.3	1113	3.3

(mm³/N m)] was calculated with the following equation:

$$w_r = \frac{\Delta m}{\rho F_N L} \quad (1)$$

where Δm is the specimen's mass loss (g), ρ is the density of the specimen (g/mm³), F_N is the normal load applied to the specimen (N), and L is the total sliding distance (m).

Morphology observation

A Philip Quanta 2000 scanning electron microscope (New York) was employed to observe the worn surface morphology of the specimens after testing. Before observation, a gold layer had to be deposited on the surface of the specimen because of the non-conductivity of the POM composites.

X-ray diffraction (XRD) experiment

Wide-angle X-ray diffraction (WAXD) patterns were obtained with a Bruker D8 Advance diffractometer (Kleve, Germany) with Ni-filtered Cu K α radiation under the following conditions: an accelerating voltage of 40 kV and an electron current of 40 mA. The scanning angle (2θ) ranged from 5 to 60°. The crystallinity degree of the POM materials was obtained with the following equation:

$$X_c = \frac{1}{1 + k(S_a/S_c)} \quad (2)$$

where X_c refers to the mass fraction crystallinity, S_c refers to the crystalline area, S_a refers to the amorphous area, and K refers to the modified coefficient (0.56).

RESULTS AND DISCUSSION

Mechanical properties

The mechanical properties of POM and its composites are listed in Table I. It can be seen that the

addition of LDPE causes a reduction in the compressive properties of POM. Among the POM/LDPE composites, the POM/7.5 wt % LDPE composite shows the best compressive properties. However, for impact strength, a maximum value of 7.2 kJ/m² was obtained for 5 wt % LDPE. On the basis of these data, in combination with the results of tribological tests (discussed in the next section), we decided to continue our study of the POM composites with the LDPE content fixed at 5 wt %.

With the further addition of RHF, the compressive properties of POM composites initially increase with the proportion of RHF but gradually decrease later. This suggests that RHF, as the reinforcing filler, plays an active role in improving the mechanical properties. However, as shown in Table I, the impact strength rapidly decreases with the proportion of RHF, which indicates that RHF reduces the toughness of POM composites. It should be noted that the incorporation of more than 7.5 wt % RHF leads to a dramatic decrease in the mechanical properties of POM, either the compressive properties or the impact strength. This could be attributed to the poor compatibility of the excessive RHF and polymer matrix, which results in a loose structure of the composite. From Table I, it can be concluded that the POM/5 wt % LDPE/5 wt % RHF composite exhibited the best general mechanical properties.

Friction and wear

The coefficient-of-friction plots as a function of the sliding distance for POM and its composites filled with LDPE and RHF are shown in Figures 2 and 3. It can be seen from Figures 2 and 3 that the coefficient of friction of POM and its composites initially decreases rapidly with a sliding distance up to 100 m and thereafter stabilizes at a steady value, which is reported as the steady-state coefficient of friction, as shown in Figures 4 and 5. This reduction in the coefficient of friction has been attributed to the

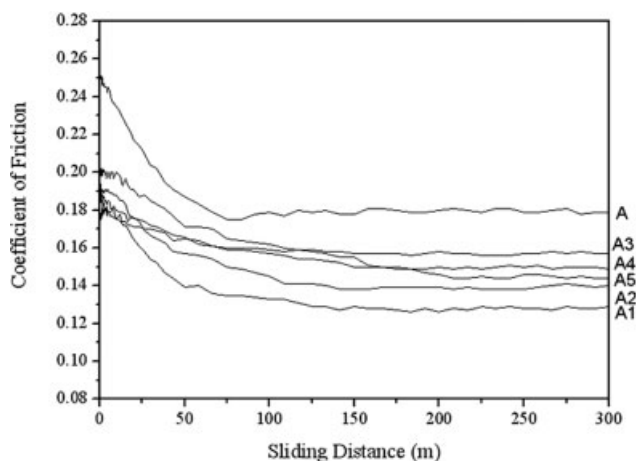


Figure 2 Variation of the coefficient of friction with the sliding distance for POM filled with LDPE (test conditions: sliding speed = 0.028 m/s and contact pressure = 5 MPa).

development of a transfer film that was observed after each test.

Figure 4 gives the steady-state coefficient of friction and wear rate of POM composites filled with various contents of LDPE. It shows that the addition of LDPE could reduce the coefficient of friction of POM. The lowest steady-state coefficient of friction of 0.126 was obtained in the case of POM/2.5 wt % LDPE, which is also the lowest value among all the POM composites tested in this study. With greater proportions of LDPE, the steady-state coefficient of friction increases to different degrees but is still lower than that of unfilled POM. To confirm this observation, the friction test for the case of 2.5 wt % LDPE was performed again, and the results coincided well with the preceding experiment. It is not very understandable why the addition of such a low

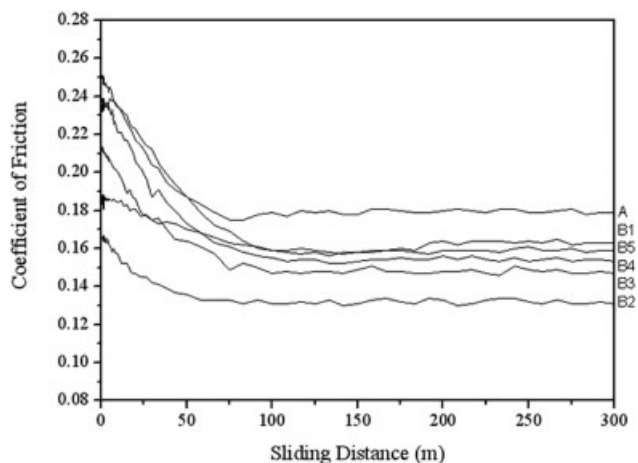


Figure 3 Variation of the coefficient of friction with the sliding distance for POM filled with both LDPE and RHF. The test conditions were the same as those in Figure 2.

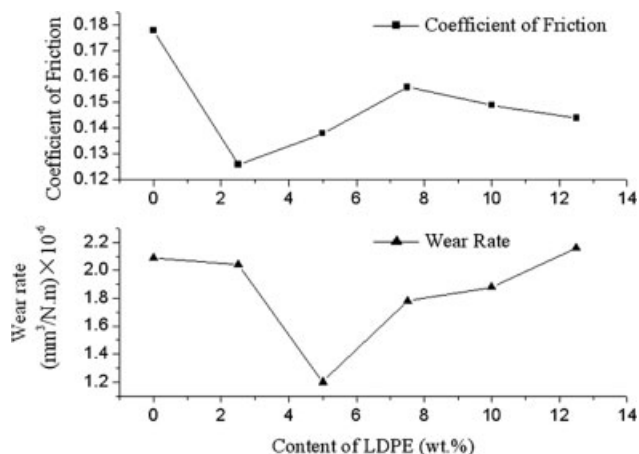


Figure 4 Variation of the steady-state coefficient of friction and wear rate with the content of LDPE for POM filled with LDPE. The test conditions were the same as those in Figure 2.

content of LDPE is much more effective in reducing the coefficient of friction than that of any other filler proportions.

As for reduction of wear, the effect of 2.5 wt % LDPE is negligibly small, but with 5 wt % LDPE, the wear rate decreases from 2.09×10^{-6} to 1.20×10^{-6} mm³/N m (a reduction by a factor of 1.7). Then, the wear rate increases rapidly with increasing LDPE content and is even higher than that of unfilled POM in the case of 12.5 wt % LDPE. This indicates that an LDPE proportion greater than 5 wt % would be undesirable in terms of wear reduction. This is presumably because the compatibility between POM and LDPE becomes weak with the proportion of LDPE larger than 5 wt %. These observations indicate that the optimum content of LDPE as the internal lubricant for POM is around 5 wt %, with which

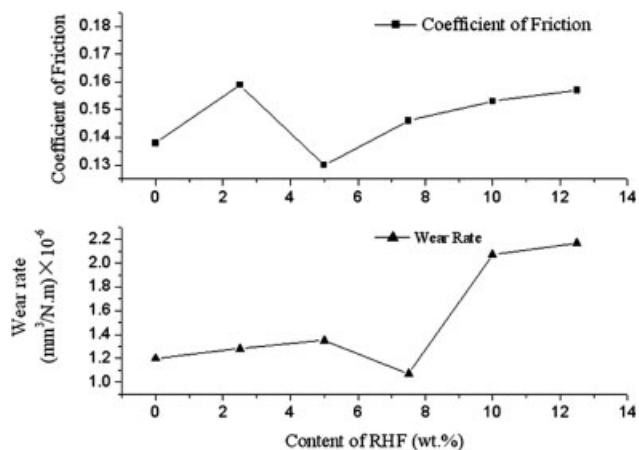


Figure 5 Variation of the steady-state coefficient of friction and the wear rate with the content of RHF for POM filled with both LDPE and RHF. The test conditions were the same as those in Figure 2.

the POM/LDPE blend has a good combination of friction and wear behavior.

Next, RHF was incorporated into the POM composites as the reinforcement, whereas the LDPE proportion was fixed at 5 wt % for the reason mentioned previously. Figure 5 shows the effect of the RHF content on the coefficient of friction and wear rate of the POM composites filled with both LDPE and RHF. The inclusion of RHF lead to an increase of different degrees in the coefficient of friction, except in the case of 5 wt % RHF. Moreover, when the RHF content is larger than 5 wt %, the coefficient of friction increases gradually with increasing RHF content. This indicates that the inclusion of RHF serves no useful purpose in reducing the coefficient of friction of POM composites in the presence of LDPE. However, it should be noted that, as can be seen from Figures 4 and 5, the coefficient of friction of POM/LDPE/RHF composites is still lower than that of unfilled POM.

It also can be seen from Figure 5 that the wear rates of the composites including 2.5 and 5 wt % RHF are close to and a little higher than that of POM/5 wt % LDPE. The lowest wear rate of $1.07 \times 10^{-6} \text{ mm}^3/\text{N m}$, among all the composites tested, has been obtained for POM/5 wt % LDPE/7.5 wt % RHF. However, when the RHF content is larger than 7.5 wt %, the wear rate of the composites dramatically increases to a value that is even comparable to that of unfilled POM. As mentioned in the earlier section, the reason might be the poor compatibility between the excessive RHF and polymer matrix, which results in a loose structure of the composite.

The aforementioned observations show that the POM/5 wt % LDPE/7.5 wt % RHF composite exhibits the best antiwear property, whereas the coefficient of friction is kept low. To further understand whether such a composite is suitable for practical applications, a comparative investigation of the tribological behaviors was made between this composite and the commercialized composites, which have been widely used in tribological applications. Friction and wear tests for these two composites were performed under the same conditions used in an earlier study. The POM/5 wt % LDPE/7.5 wt % RHF composite has a wear rate lower than that of POM/20 wt % PTFE but a little higher than that of POM/20 wt % PTFE/10 wt % glass fiber (GF). The POM/5 wt % LDPE/7.5 wt % RHF composite exhibits a coefficient of friction lower than that of the POM/20 wt % LDPE/10 wt % RHF composite but higher than that of POM/20 wt % PTFE. In other words, the POM/5 wt % LDPE/7.5 wt % RHF composite has a better combination of friction and wear behavior than either of the two composites. Thus, it is supposed that this composite is a potential material for practical applications.

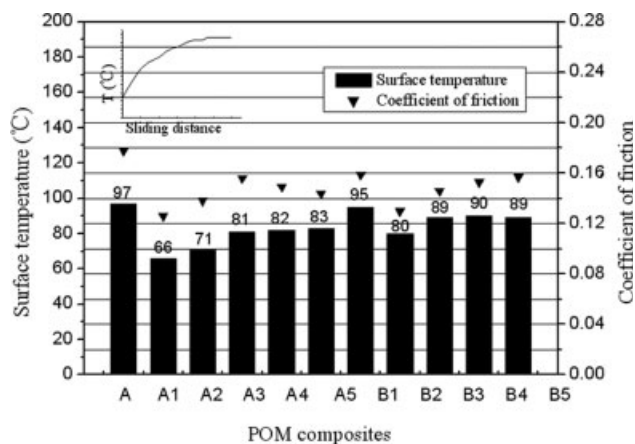


Figure 6 Surface temperatures of POM and its composites after the 300-m friction and wear test.

Surface temperature

The surface temperature of POM and its composites after the 300-m friction and wear test is presented in Figure 6, and a schematic diagram of the trend of changes in the surface temperature during the test is also shown in the top left corner of Figure 6. In addition, the coefficient of friction of POM and its composites is given in Figure 6 to further understand the interrelationship between the surface temperature and tribological behaviors of POM composites.

It is distinct that the two parameters (surface temperature and coefficient of friction) are closely correlated with each other. There is a general tendency that the larger the coefficient of friction is, the higher the surface temperature is. It is not difficult to understand that increasing the coefficient of friction leads to an increase in the frictional heat, which mainly determines the surface temperature. However, the tendency is not so clear in the case of a high filler content. This is presumably because excessive filler greatly affects the thermal properties (e.g., thermal conductivity) of POM composites, which also play an important role in determining the surface temperature. The same explanation could be given for the following phenomenon: as can be seen from Figure 6, the surface temperature of composites B3, B4, and B5 is obviously higher than that of composites A3, A4, and A5, although the coefficients of friction for these composites are comparable. It is believed that the poor thermal conductivity of RHF is responsible for the rise in the surface temperature. No apparently direct connection has been found between the surface temperature and wear rate. It could not be said, nevertheless, that there is no relationship between the two. This is because the surface temperature rise could greatly affect the mechanical properties of polymer composites and consequently influence the wear performance, especially when the

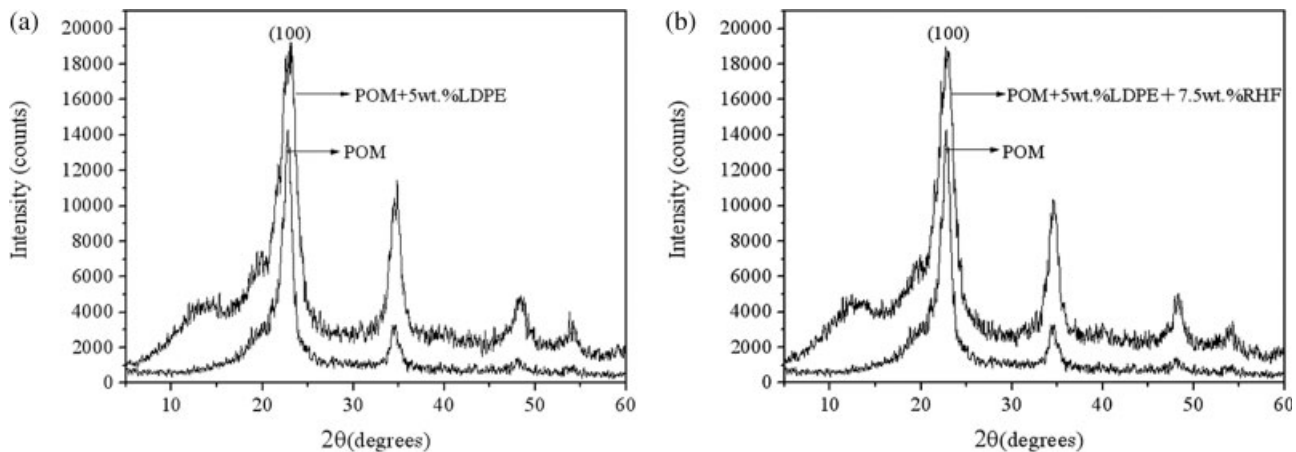


Figure 7 XRD patterns of POM and its typical composites.

flash temperature at the asperity peaks of the real contact area is considered.¹⁶

XRD analysis

Figure 7 presents the XRD patterns of POM and its composites. The two strong diffraction peaks at $2\theta = 22.8^\circ$ and $2\theta = 34.7^\circ$ are the distinctive feature of the hexagonal crystalline form of POM. For POM composites, the diffraction angle almost remains unchanged, and this indicates that the filler does not change the crystalline form of the POM matrix. As expected, the intensity of the diffraction peaks increases with the addition of filler. What is more important, the fraction peaks of the POM composites broaden, indicating less crystallinity perfection.

To obtain more information about the crystallinity perfection, the crystallinity degree of POM and its composites was calculated from the amorphous and crystalline areas of the POM (100) diffraction peak, corresponding to a modified coefficient of $k = 0.56$ in eq. (2).¹⁷ The results are listed in Table II. There is a noticeable decrease of about 10% points in the crystallinity degree for the POM/LDPE composites compared to unfilled POM. With the addition of RHF, the crystallinity degree is further slightly lowered. The lowest crystallinity degree of 56.2%, a reduction of 12.9 percentage points compared to that of unfilled POM, is found for the POM/5 wt % LDPE/12.5 wt % RHF composite. The possible reason for the reduction in the crystallinity degree is that the presence of the filler restrains the crystallization process of POM to a certain extent.

Table II also shows that the crystallinity degree of the composites changes very little with the content of the filler, either LDPE or RHF. Consequently, it is important to point out that the crystallinity degree should not be considered the main factor that affects the mechanical and tribological behaviors of POM composites in this study, although an increasing crystallinity degree

often brings better mechanical properties and sometimes even better tribological behaviors.¹⁸

Examination of worn surfaces

Figures 8–10 show the scanning electron microscopy (SEM) morphologies of the worn surfaces of POM and its typical composites. Figure 8(a) shows that for unfilled POM, the abrasion marks parallel to the sliding direction are not as clear as in the case of POM composites, and severe plastic deformation and adhesion can be clearly seen with higher magnification [Fig. 8(b)]. These observations suggest that the wear process of unfilled POM is governed by an adhesive wear mechanism. In fact, the unfilled POM exhibited the highest surface temperature of 97°C during the steady-state sliding. Such a high temperature, together with the heavy loading condition, led to the softening of POM in the real contact area where a higher flash temperature was expected. As a result, severe plastic deformation and adhesion occurred, resulting in POM materials being rapidly removed by the hard asperities of the metallic counterface.

TABLE II
Calculated WAXD Results of POM and Its Composites

POM composite	Amorphous area [$C_{ps} \times 2\theta$ ($^\circ$)]	Crystalline area [$C_{ps} \times 2\theta$ ($^\circ$)]	Crystallinity degree (%)
A	16,494.3	20,690.3	69.1
A1	43,001.1	36,314.7	60.1
A2	41,236.3	36,586.9	61.3
A3	42,482.1	36,122.8	60.3
A4	44,737.3	34,439.5	57.9
A5	43,197.8	36,791.9	60.3
B1	42,235.5	34,240.0	59.1
B2	41,882.2	31,648.1	57.4
B3	43,182.2	34,002.1	58.4
B4	44,771.2	32,310.0	56.3
B5	44,731.1	32,088.1	56.2

C_{ps} , counts per second.

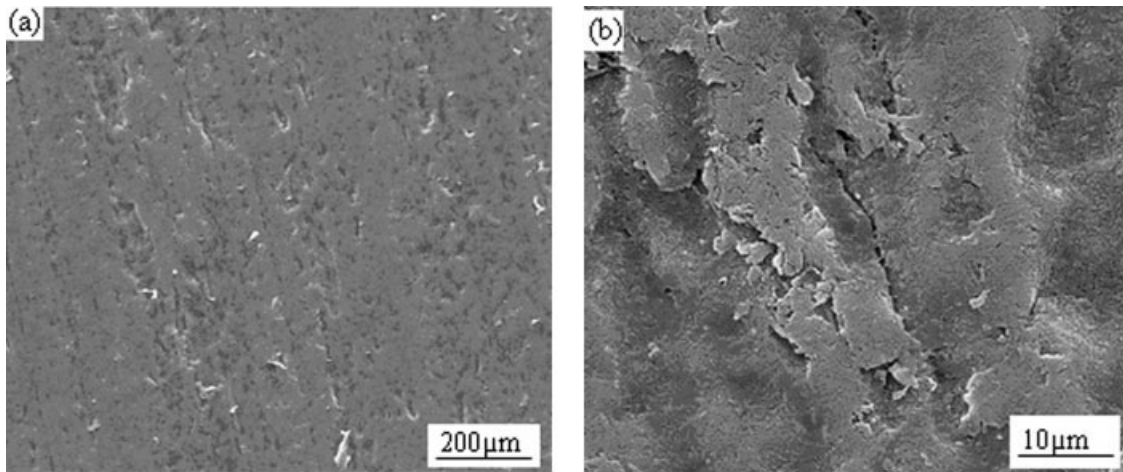


Figure 8 SEM micrographs of the worn surface of unfilled POM.

Figure 9 shows that the worn surfaces of the POM composites filled with LDPE are relatively smooth compared to that of unfilled POM. Even at a high

magnification, plastic deformation can barely be seen [Fig. 9(b,d)]. Figure 9(b) also shows that there is some tiny wear debris adhering to the worn surface

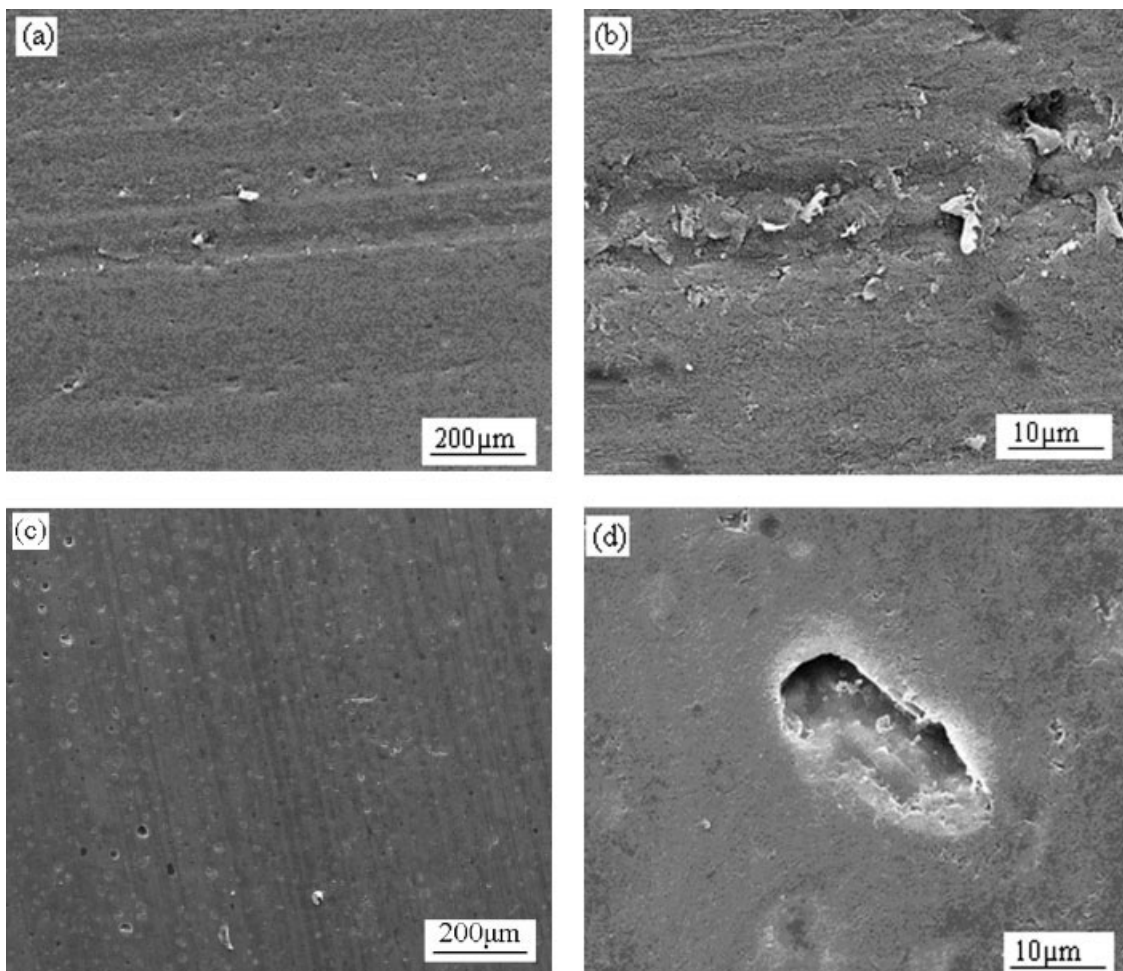


Figure 9 SEM micrographs of the worn surfaces of the POM composites filled with LDPE alone: (a,b) 5 and (c,d) 12.5 wt % LDPE.

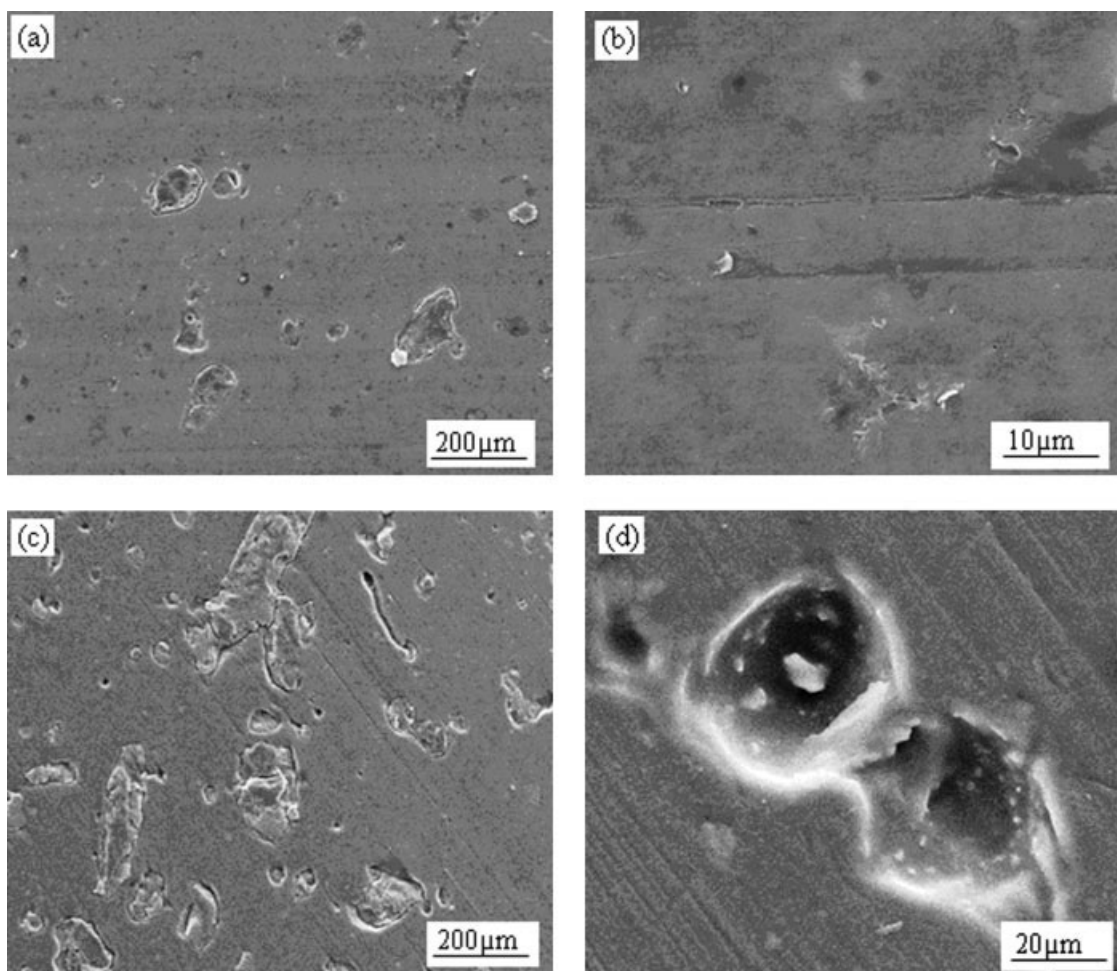


Figure 10 SEM micrographs of the worn surfaces of the POM composites filled with both LDPE and RHF: (a,b) 7.5 and (c,d) 12.5 wt % RHF.

of the POM/5 wt % LDPE composite, which agrees with its low wear loss. In the case of 12.5 wt % LDPE, as can be seen in Figure 9(d), a local wear scar was observed on the worn surface, which could lead to large wear debris and consequently high wear loss. It is supposed that such a large wear scar was caused by the fatigue wear of adhesive contact.¹⁹ As discussed earlier in this article, excessive LDPE addition could result in a weak bond between the POM matrix and LDPE, so microcracks may occur and expand under the repeated sliding action.

For the composites including RHF, well-distributed RHF can be clearly seen on the worn surface [Fig. 10(a,c)]. With a high magnification, as can be seen in Figure 10(b), no obvious damage could be found on the worn surface of POM/5 wt % LDPE/7.5 wt % RHF, except for some nanogrooves parallel to the sliding direction. These grooves are much slighter than those of the POM/5 wt % LDPE composite [Fig. 9(a)], indicating that 7.5 wt % RHF acts effectively as the reinforcement for POM. Therefore, for this composite, which has the lowest wear rate

among all the composites tested, wear presumably occurred by fatigue and the depletion of transfer film.^{20,21} In the case of 12.5 wt % RHF, large cavities, which were caused by the removal of RHF due to the repeated sliding action, were observed [Fig. 10(d)]. This observation confirms the assumption proposed in the earlier section that excessive RHF could lead to a loose structure of the POM composite due to the poor compatibility between the matrix and RHF.

CONCLUSIONS

1. The impact strength of POM composites filled with LDPE increases with filler addition up to 5 wt %, and the compressive properties decrease because of the addition of LDPE. The POM/5 wt % LDPE/5 wt % RHF composite showed good mechanical strength.
2. The addition of the proper content of LDPE increases the tribological behaviors of POM. The POM/5 wt % LDPE composite showed a

good combination of friction and wear behaviors, The lowest wear rate of $1.07 \times 10^{-6} \text{ mm}^3/\text{N m}$ was obtained for POM/5 wt % LDPE/7.5 wt % RHF. An SEM examination of the worn surfaces revealed that the main wear mechanism for unfilled POM is adhesion. As for POM composites, wear seems to occur mainly by fatigue and abrasion.

3. It was experimentally confirmed that it is feasible to produce a POM composite for tribological applications that is well-performing, low-cost, and environmentally friendly.

References

1. TonPeijs. *e-Polymers* 2002, 2, 1.
2. Linton, J.; Yeomans, J. S. *Nat Mater* 2004, 3, 199.
3. Saheb, D. N.; Jog, J. P. *Adv Polym Tech* 1999, 18, 351.
4. Daniel, F. C.; Daan, F.; Prabawa, S.; Young, R. A.; Anand, R. S. *Angew Makromol Chem* 1999, 272, 57.
5. Tajvidi, M.; Falk, R. H.; Hermanson, J. C. *J Appl Polym Sci* 2006, 101, 4341.
6. Facca, A. G.; Kortschot, M. T.; Yan, N. *Compos Sci Technol* 2007, 67, 2454.
7. Bledzki, A. K.; Gassan, J. *Prog Polym Sci* 1999, 24, 221.
8. Joseph, P. V.; Rabello, M. S.; Mattoso, L. H. C.; Joseph, K.; Thomas, S. *Compos Sci Technol* 2002, 62, 1357.
9. Canché-Escamilla, G.; Rodriguez-Laviada, J.; Cauich-Cupul, J. I.; Mendizábal, E.; Puig, J. E.; Herrera-Franco, P. J. *Compos A* 2002, 33, 539.
10. O'Donnell, A.; Dweib, M. A.; Wool, R. P. *Compos Sci Technol* 2004, 64, 1135.
11. Wu, J.; Yu, D.; Chan, C.; Kim, J.; Mai, Y. *Compos Sci Technol* 2006, 66, 13188.
12. Magurno, A. *Angew Makromol Chem* 1999, 272, 99.
13. Odi-Owei, S.; Schipper, D. J. *Wear* 1991, 148, 363.
14. Kurokawa, M.; Uchiyama, Y.; Nagai, S. J. *J Tribol* 2000, 122, 809.
15. Benabdallah, H. *Wear* 2003, 254, 1239.
16. Guha, D.; Roy Chowdhuri, S. K. *Wear* 1996, 197, 63.
17. Wu, R. J. *Modern Analytical Techniques*; Shanghai Science and Technology: Shanghai, 1987.
18. Xiang, D.; Tao, K. *J Appl Polym Sci* 2007, 103, 1035.
19. Chang, L.; Chang, Z.; Zhang, H.; Schlarb, A. K. *Compos Sci Technol* 2006, 66, 3188.
20. Shangguan, Q. Q.; Cheng, X. H. *Wear* 2006, 260, 1243.
21. Cho, M. H.; Bahadur, S. *Wear* 2005, 258, 835.